


**Steady-state entropy: A proposal based on thermodynamic integration**

Leonardo Ferreira Calazans\* and Ronald Dickman†

*Departamento de Física and National Institute of Science and Technology for Complex Systems, ICEx, Universidade Federal de Minas Gerais, C.P. 702, 30123-970 Belo Horizonte, Minas Gerais, Brazil* (Received 16 February 2018; revised manuscript received 13 December 2018; published 28 March 2019)

Defining an entropy function out of equilibrium is an outstanding challenge. For stochastic lattice models in spatially uniform nonequilibrium steady states, definitions of temperature  $T$  and chemical potential  $\mu$  have been verified using coexistence with heat and particle reservoirs. For an appropriate choice of exchange rates,  $T$  and  $\mu$  satisfy the zeroth law, marking an important step in the development of *steady-state thermodynamics*. These results suggest that an associated steady-state entropy  $S_{th}$  be constructed via thermodynamic integration, using relations such as  $(\partial S/\partial E)_{V,N} = 1/T$ , ensuring that derivatives of  $S_{th}$  with respect to energy and particle number yield the expected intensive parameters. We determine via direct calculation the stationary nonequilibrium probability distribution of the driven lattice gas with nearest-neighbor exclusion, the Katz-Lebowitz-Spohn driven lattice gas, and a two-temperature Ising model so that we may evaluate the Shannon entropy  $S_S$  as well as  $S_{th}$  defined above. Although the two entropies are identical in equilibrium (as expected), they differ out of equilibrium; for small values of the drive,  $D$ , we find  $|S_S - S_{th}| \propto D^2$ , as expected on the basis of symmetry. We verify that  $S_{th}$  is *not a state function*: changes  $\Delta S_{th}$  depend not only on the initial and final points, but also on the path in parameter space. The inequivalence of  $S_S$  and  $S_{th}$  implies that derivatives of  $S_S$  are not predictive of coexistence. In other words, a nonequilibrium steady state is not determined by maximizing the Shannon entropy. Our results cast doubt on the possibility of defining a state function that plays the role of a thermodynamic entropy for nonequilibrium steady states.

DOI: [10.1103/PhysRevE.99.032137](https://doi.org/10.1103/PhysRevE.99.032137)**I. INTRODUCTION**

A fundamental question in physics and chemistry concerns the possibility of formulating a far-from-equilibrium thermodynamics. Since the notions of irreversibility and approach to equilibrium rest on the postulate that the entropy of a closed system cannot decrease, it is paradoxical that a general definition of entropy out of equilibrium is not available. For systems in *local equilibrium*, the thermodynamic entropy  $S_{th}$  is given integrating the equilibrium entropy density over space, so that  $S_{th}$  becomes a functional of the slowly varying temperature and chemical potential fields. But this definition does not apply far from equilibrium. Given the simplicity of Shannon entropy  $S_S$  as a functional of the probability distribution on phase space, its equality with  $S_{th}$  in equilibrium, and the lack of alternatives,  $S_S$  is often used as the entropy out of equilibrium as well [1–7]. By contrast, Komatsu *et al.* [8], construct extensions of state functions from equilibrium to nonequilibrium steady states (NESSs), and find that the entropy for a NESS differs from the Shannon form. We note however that the approach of [8] is quite different from that adopted in the present work, which is based on intensive parameters defined operationally, via coexistence.

By thermodynamics we understand a closed description using a small number of macroscopic quantities, capable of

predicting the state of a system when some constraint is removed [9]. There are currently two main approaches to this issue: *stochastic thermodynamics* [5,10–12], and *steady-state thermodynamics* (SST) [12–15]. The latter was proposed by Oono and Paniconi [13], applied to Langevin systems [16] and driven lattice gases [17], and further developed and applied to several models by Sasa and Tasaki [14]. General expressions for intensive parameters were derived by Bertin *et al.* [18]. The consistency of the definition of intensive parameters has been tested numerically and partially verified [19,20]. The notions of intensive parameters and coexistence in nonequilibrium steady states were further developed by Chatterjee *et al.* [21,22]. Recently, consistent definitions of temperature and chemical potential were verified for uniform driven lattice gases in NESSs; the chemical potential correctly predicts the densities of coexisting steady states [23]. The approaches to SST mentioned above are based (as is the present work) on defining intensive parameters; the entropy would then be obtained via thermodynamic integration. An alternative approach eschews the use of intensive parameters far from equilibrium, and is instead based on the (Shannon) entropy [10–12].

While a complete far-from-equilibrium thermodynamics should, in principle, include a definition of the entropy, this is a daunting task, and many studies have focused instead on defining intensive variables such as temperature  $T$  and chemical potential  $\mu$  [14,20,23]. Once an intensive variable has been determined, it is of interest to ask whether the entropy  $S$  can be obtained (up to a constant) by integrating

\*leonardo.ferreira.calazans@gmail.com

†dickman@fisica.ufmg.br

one of the standard thermodynamic relations, for example,

$$S_{th}(E) = \int_{E_0}^E \frac{dE'}{T(E')} + S_0(E_0, N, V), \quad (1)$$

where  $E$ ,  $N$ , and  $V$  denote internal energy, particle number, and volume. We call  $S_{th}(E)$  the *thermodynamic* entropy (as opposed to, say, information entropy), since by construction its derivative yields an intensive thermodynamic parameter that can be used to predict coexistence between systems. Summarizing, we define intensive variables via coexistence, in a manner consistent with the zeroth law, and attempt to construct an entropy function via thermodynamic integration involving the intensive variables so obtained.

In this work we examine the feasibility of this approach to defining a steady-state entropy in simple lattice models with stochastic dynamics. The models studied all violate global detailed balance, so that the stationary probability distribution on configuration space is not the Boltzmann distribution. Using an exact (numerical) solution of the master equation, we obtain the stationary probability distribution, and then calculate the change  $\Delta S_{th}$  for a given path in parameter space. Comparing the changes for two paths between the same initial and final points, we test whether  $S_{th}$  is a state function. We also examine whether  $S_{th}$  is equal to the Shannon entropy  $S_S$ . Information on the latter quantity for NESSs is extremely limited, since it requires evaluation of the stationary probability distribution  $P$  on configuration space. Here we use a numerically exact method to calculate  $P$  for small systems of interacting particles or spins. We find that  $S_{th}$  is *not* a state function out of equilibrium. While one might be tempted to attribute this result to our definitions of intensive variables  $T$  and  $\mu$ , we note that the latter follow directly from the principle of zero net flux between systems that share the same values of these variables, which is a cornerstone of thermodynamics. Since  $S_{th}$  is not a state function out of equilibrium, it cannot be equal to the Shannon entropy, which is always a state function. This implies that equating the derivatives  $S_S$  *does not predict coexistence between nonequilibrium steady states*, or, equivalently, that nonequilibrium steady states are not determined by maximizing the Shannon entropy. [Different from equilibrium, it is not possible, for example, to predict the coexistence energies of systems  $A$  and  $B$ , with fixed total energy  $E = E_A + E_B$ , by maximizing  $S_{S,A}(E_A) + S_{S,B}(E - E_A)$ .] Without a state function whose derivatives yield the intensive parameters associated with coexistence, there is no thermodynamic steady-state entropy out of equilibrium.

The remainder of this paper is organized as follows. In Sec. II we define the models to be investigated, and explain how the relevant intensive parameter (chemical potential or temperature) is determined. In Sec. III we explain our numerical method for determining the stationary probability distribution. Section IV presents our results, followed in Sec. V by a summary and discussion.

## II. MODELS

We consider the following stochastic lattice models in order to compare thermodynamic and Shannon entropies. All the models studied here are implemented on  $L \times L$  square lattices with periodic boundaries.

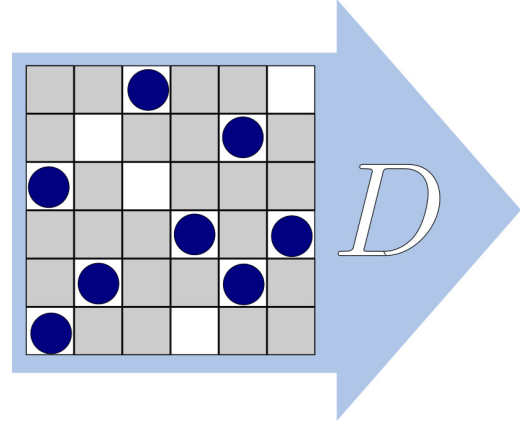


FIG. 1. Schematic of NNE lattice gas. Dark circles denote particles, white squares, open sites. Grey squares are nonopen vacant sites.  $\mathbf{D}$  denotes the drive.

### A. Driven lattice gas with nearest-neighbor exclusion (NNE model) [24]

Each site may be either vacant or occupied by a particle, with occupation of nearest-neighbor pairs prohibited (see Fig. 1). All allowed configurations possess the same energy, marking this as an athermal model; in equilibrium all are equally probable. A consequence of the athermal nature of this model is that the only intensive parameter is the dimensionless chemical potential,  $\mu^* = \mu/k_B T$  ( $\mu$  is defined in Appendix A), which is a function of  $N$  and  $L$ , or of the density  $\rho = N/L^2$  in the thermodynamic limit. (From here on, we set Boltzmann's constant  $k_B = 1$ .) The configuration evolves via a particle-conserving, continuous-time Markovian dynamics of single-particle jumps to first or second neighbor sites, i.e., displacements of the form  $\Delta \mathbf{x} = \sigma \mathbf{i} + \eta \mathbf{j}$ , with  $\sigma \in \{-1, 0, 1\}$ , and similarly for  $\eta$ , excluding  $\sigma = \eta = 0$ . (Here,  $\mathbf{i}$  and  $\mathbf{j}$  denote unit vectors along the positive  $x$  and  $y$  directions, respectively.) Each particle has the same probability ( $1/N$ ) to be the next to attempt to hop. In the presence of a drive  $\mathbf{D} \equiv D \mathbf{i}$ , the displacement probabilities are

$$P_{\text{hop}}(\sigma \mathbf{i} + \eta \mathbf{j}) = \frac{1 + \mathbf{D} \cdot \Delta \mathbf{x}}{8} = \frac{1 + \sigma D}{8}. \quad (2)$$

Thus  $D = 0$  corresponds to equilibrium, while  $D = 1$  corresponds to maximum drive, with jumps in the  $-x$  direction prohibited. Any particle displacement yielding a configuration satisfying the NNE condition is accepted; otherwise it is rejected and the system remains in the current configuration. The stationary probability distribution can be calculated numerically from the master equation for small systems (up to  $L = 7$  in the present study). For  $L$  even and  $N$  close to  $L^2/2$  (the maximum particle number), this dynamics admits frozen configurations, in which no particle is free to move. (Such configurations are likewise inaccessible from nonfrozen configurations.) We avoid classes  $(L, N)$  values for which frozen configurations exist.

In the NNE lattice gas, a site is *open* if it and all its nearest neighbors (NNs) are vacant; particles can only be inserted at open sites. Since we work at fixed volume and all configurations possess the same energy, the parameter space

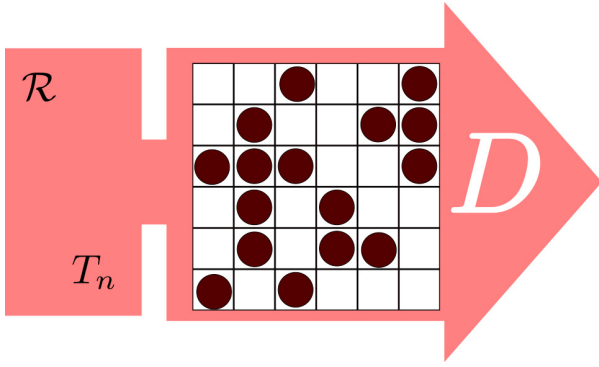


FIG. 2. Schematic of KLS lattice gas. Dark circles denote particles, **D** the drive. Hopping probabilities involve the parameter  $T_n$ , associated with a reservoir  $\mathcal{R}$ . For nonzero drive, there is a steady transfer of energy from the drive to the lattice gas, and from the latter to  $\mathcal{R}$ .

is restricted to the possible values of  $N$ , and the issue of path independence does not arise in this case.

As shown in Appendix A, the thermodynamic and Shannon entropies can only be equal if

$$\begin{aligned} \sum_{\mathcal{C} \in \Gamma(L, N)} P(\mathcal{C}) \ln P(\mathcal{C}) - \sum_{\mathcal{C} \in \Gamma(L, N-1)} P(\mathcal{C}) \ln P(\mathcal{C}) \\ = \ln \frac{\bar{N}_{op}(L, N-1)}{N}, \end{aligned} \quad (3)$$

where  $P(\mathcal{C})$  is the stationary probability distribution,  $\bar{N}_{op}(L, N)$  is the stationary average of the number of open sites in a system of  $L^2$  sites with  $N$  particles, and  $\Gamma(L, N)$  is the associated configuration space. Any violation of this relation implies that the Shannon and thermodynamic entropies are unequal.

### B. Driven lattice gas with nearest-neighbor attractive interactions or Katz-Lebowitz-Spohn (KLS) model

The KLS model [25–27], is a stochastic lattice gas in which each site  $i$  of a lattice is either vacant (occupation variable  $\sigma_i = 0$ ) or occupied ( $\sigma_i = 1$ ). The number of particles  $N$  is conserved (see Fig. 2). Hence in this case  $\Gamma(L, N)$  consists of all configurations in which exactly  $N$  sites of an  $L \times L$  lattice are occupied. The interaction energy is

$$E = - \sum_{(i, j)} \sigma_i \sigma_j, \quad (4)$$

where the sum is over NN pairs of sites; each NN particle pair lowers the energy by one unit. In equilibrium, this system is equivalent to the NN ferromagnetic Ising model with conserved magnetization. Transitions between configurations in the KLS model occur via hopping of particles to NN sites. (Each hopping event involves movement of a single particle.) A nonequilibrium drive  $\mathbf{D} = D\mathbf{i}$  favors displacements along the  $+x$  direction, and suppresses those in the opposite sense. The acceptance probability for a particle displacement  $\Delta \mathbf{x}$  is

$$p_a(\Delta \mathbf{x}) = \min\{1, \exp[-(\Delta E - D\mathbf{i} \cdot \Delta \mathbf{x})/T_n]\}, \quad (5)$$

where  $T_n$  is the “nominal” temperature, i.e., that of a reservoir that exchanges energy with the particle system. (In the steady state, the particle system gains energy from the drive and transfers, on average, an equal quantity of energy per unit time to this reservoir [23].)

We determine the thermodynamic temperature  $T$  of a KLS model  $\mathcal{S}$  in its stationary state via virtual contact with a heat reservoir  $\mathcal{R}$ . (Note that in equilibrium,  $T = T_n$  but that for nonzero drive,  $T > T_n$ .) Interaction between  $\mathcal{S}$  and  $\mathcal{R}$  does not involve the drive, only the configurational energy  $E$ . Let  $w(\Delta E)$  be the rate at which the reservoir stimulates transitions in  $\mathcal{S}$  with energy change  $\Delta E$ . The defining property of the reservoir is

$$w(\Delta E) = e^{-\Delta E/T} w(-\Delta E). \quad (6)$$

There are, of course, many functions  $w(\epsilon)$  that satisfy Eq. (6); here we use Sasa-Tasaki (ST) rates [14], since they lead to a definition of temperature consistent with the zeroth law [23]. The ST rate for a transition from configuration  $\mathcal{C}$  to  $\mathcal{C}'$  depends only on the energy of the hopping particle in the initial configuration  $\mathcal{C}$ . This means that if  $\mathcal{C}'$  is accessible from  $\mathcal{C}$  via displacement of particle  $j$ , then

$$w_{ST}[\mathcal{C} \rightarrow \mathcal{C}'] = w_0 \exp[E_j(\mathcal{C})/T], \quad (7)$$

where  $w_0$  is an arbitrary fixed rate, and  $E_j(\mathcal{C})$  is the energy of interaction between particle  $j$  and its neighbors in configuration  $\mathcal{C}$ , that is,  $-m_j$ , with  $m_j$  the number of occupied NNs of particle  $j$ . (Note that in the KLS model, if  $\mathcal{C}'$  is accessible from  $\mathcal{C}$ , then  $\mathcal{C}$  is accessible from  $\mathcal{C}'$ .)

To determine the thermodynamic temperature of system  $\mathcal{S}$  we must find the value of  $T$  such that the stationary net energy flux between  $\mathcal{S}$  and  $\mathcal{R}$  is zero, that is

$$\begin{aligned} J_E = \frac{w_0}{2} \sum_{\mathcal{C}, \mathcal{C}'} [E(\mathcal{C}') - E(\mathcal{C})] [e^{E_j(\mathcal{C})/T} P(\mathcal{C}) - e^{E_j(\mathcal{C}')/T} P(\mathcal{C}')] \\ = 0, \end{aligned} \quad (8)$$

where the sum is over all pairs of configurations  $\mathcal{C}$  and  $\mathcal{C}'$  such that  $\mathcal{C}'$  is accessible from  $\mathcal{C}$ . Then, knowing the internal energy  $E(T)$  (given, naturally, as an average over the stationary probability distribution), we can determine  $S_h$  using Eq. (1).

The parameter space  $(T_n, N)$  for the KLS model at fixed volume is two dimensional, so that we may compare entropy changes associated with different paths between the same initial and final points. As shown in Appendix B of Ref. [14], the dimensionless chemical potential of a lattice gas with attractive NN interactions is

$$\mu^*(\beta, N) = \ln \frac{g}{1 - \rho}, \quad (9)$$

where  $g = \sum_{j=0}^q \rho^-(j) e^{-\beta j}$ , with  $\rho^-(j)$  the steady-state average density (in the system with  $N$  particles) of occupied sites that have exactly  $j$  occupied NNs. Here  $\beta$  is the inverse temperature of the heat reservoir that coexists with the system. (Recall that for nonzero drive,  $\beta \neq 1/T_n$ .) In a finite system, the denominator must be taken as  $1 - \rho = 1 - (N-1)/L^d$ , in  $d$  dimensions, as shown below in Appendix A. At fixed temperature, the chemical potential represents the difference in Helmholtz free energy,  $A = E - TS$ , between the system with  $N$  particles and that with  $N-1$ . Thus we write for the

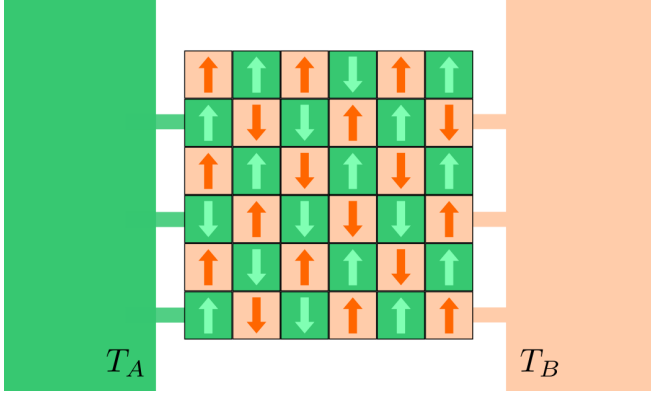


FIG. 3. Schematic of two-temperature Ising model. Sites in the sublattices  $A$  and  $B$  (arranged in a checkerboard pattern) are in contact with reservoirs at temperature  $T_A$  and  $T_B$ .

entropy

$$S(\beta, N) - S(\beta, N - 1) = -\mu(\beta, N) + \beta[E(\beta, N) - E(\beta, N - 1)], \quad (10)$$

where  $E(\beta, N)$  and  $E(\beta, N - 1)$  are the mean energies, evaluated at the same value of  $\beta$ . Now, the right-hand side (r.h.s.) of Eq. (10) represents the entropy change on inserting a particle. The left-hand side (l.h.s.) can be calculated via an alternative path, i.e., using Eq. (1) for particle numbers  $N$  and  $N - 1$ . In the  $T$ - $N$  plane, the l.h.s. corresponds to the sum of entropy changes along three lines: (i) from  $T$  to  $T = \infty$  at fixed particle number,  $N - 1$ ; (ii) from  $N - 1$  to  $N$  at infinite temperature; (iii) from  $T = \infty$  to  $T$  at fixed particle number  $N$ . The r.h.s. corresponds to jumping from  $N - 1$  to  $N$  at fixed temperature  $T$ . If the two expressions for  $S(\beta, N) - S(\beta, N - 1)$  disagree, the entropy change is path dependent.

### C. Two-temperature Ising model (TTI)

In the two-temperature Ising model [28,29], the interaction energy is again given by Eq. (4), but with  $\sigma_i$  now a *spin* variable, taking values  $\pm 1$  (see Fig. 3). The configuration space  $\Gamma(L)$  corresponds to all  $2^{L^2}$  possible assignments of spin variables. The stochastic evolution proceeds via spin flips ( $\sigma_i \rightarrow -\sigma_i$ ), with transition rates

$$w(\sigma_i \rightarrow -\sigma_i) = \exp \left[ -\beta_i \sigma_i \sum_{j \text{ NN } i} \sigma_j \right], \quad (11)$$

where the sum is over the nearest neighbors  $j$  of site  $i$ .

Since there is no preferred direction, there is no particle (or spin) current in the TTI. In this case the nonequilibrium condition arises from having sites in different sublattices in contact with reservoirs at distinct temperatures. Specifically, let sublattice  $A$  correspond to sites  $(i, j)$  such that  $i + j$  is even, and let sublattice  $B$  contain those with  $i + j$  odd. (On the square lattice, all neighbors of a site in  $A$  lie in  $B$ , and vice versa.) In the transition rate, Eq. (11),  $\beta_i = \beta_A = 1/T_A$  for flipping a spin in sublattice  $A$ , while the flip rate in sublattice  $B$  involves  $\beta_B$ ; thus  $T_A = T_B$  corresponds to the equilibrium Ising

model. For  $T_A \neq T_B$  the system cannot reach equilibrium; there is a net flux of energy from the hotter to the colder sublattice. Determination of the thermodynamic temperature and entropy follows the same procedure as in the KLS model. In this case we probe path independence in the  $T_A$ - $T_B$  plane.

### III. METHODS

To implement our definition of  $S_{th}$ , test its path independence, and compare it with the Shannon entropy, we require the stationary probability distribution on configuration space  $P(\mathcal{C})$ . In this section we provide some details on how we obtain the stationary solution of the master equation using the method developed in [30,31].

To reduce the computational effort, in place of configurations, we consider classes of configurations that are equivalent under lattice translations. Given the periodic boundaries, all members of such an equivalence class have the same stationary probability. Moreover, since we use an initial distribution that is uniform on configuration space, equality of probability for all configurations in the same class holds at all times. Let  $\mathcal{C}_1$  and  $\mathcal{C}_2$  be two configurations in  $\Gamma(L, N)$ . We say that  $\mathcal{C}_2$  belongs to the same equivalence class of  $\mathcal{C}_1$  if there is a lattice translation, denoted by  $\mathcal{T}$ , such that  $\mathcal{C}_2 = \mathcal{T}(\mathcal{C}_1)$ . For each class  $\chi$ , we store a representative configuration and the number of configurations in the class,  $\omega(\chi)$ .

It is convenient to write the master equation for  $p(\mathcal{C}, t)$  in the form

$$\dot{p}(\mathcal{C}, t) = -w(\mathcal{C})p(\mathcal{C}, t) + r(\mathcal{C}, t), \quad (12)$$

where

$$r(\mathcal{C}, t) = \sum_{\mathcal{C}'} w[\mathcal{C}' \rightarrow \mathcal{C}] p(\mathcal{C}', t) \quad (13)$$

and

$$w(\mathcal{C}) = \sum_{\mathcal{C}'} w[\mathcal{C} \rightarrow \mathcal{C}']. \quad (14)$$

Since we work with classes of configurations equivalent under translations, we can analyze a system of equations of this form using just one representative of each class, rather than one for each configuration.

To set up the master equation, we first enumerate all configurations in  $\Gamma(L, N)$  and assign them to equivalence classes. Then, for each class, we enumerate all possible transitions (and their corresponding rates) originating from the representative configuration, determining the class to which the new configuration belongs. These data, as well as the exit rates  $w(\mathcal{C})$ , are stored in lookup tables.

To determine the stationary probability distribution, we use the iterative numerical method described in [30]. Starting from a uniform initial distribution, the  $k$ th estimate  $p^k(\mathcal{C})$  is obtained via

$$p^k(\mathcal{C}) = ap^{k-1}(\mathcal{C}) + (1-a) \frac{r^{k-1}(\mathcal{C})}{w(\mathcal{C})}, \quad (15)$$

where  $r^{k-1}$  denotes Eq. (13) evaluated using the probability distribution at step  $k-1$ . Here,  $a$  is a parameter in the interval  $(0, 1)$ . Smaller values of  $a$  yield faster convergence, but may also lead to numerical instability; in the present work we use

$a = 0.5$ . As a stopping criterion, we use the stabilization of the Shannon entropy of  $p(C)$ . Specifically, we halt the iterative process when  $|S_S^k - S_S^{k-1}| \leq 10^{-10}$ .

**IV. RESULTS**

**A. Lattice gas with NNE**

We applied the method described above to the driven NNE lattice gas with  $L = 4-7$ . In the present study, the case with the largest number of configuration classes is  $L = 7$  and  $N = 11$ , for which there are 1 906 532 classes and 58 744 440 transitions. In this case the probability distribution converges after 115 iterations.

Varying  $L$  and  $N$ , we verify in all cases that in equilibrium (drive  $D = 0$ ), Eq. (3) is satisfied to a precision of one part in  $10^{10}$ . The identity is violated, however, for  $D \neq 0$ . It is convenient to define

$$V(L, N) \equiv \left| \ln \frac{\bar{N}_{op}(L, N - 1)}{N} - \Delta S_S(L, N) \right| \quad (16)$$

to quantify the difference between changes in Shannon and thermodynamic entropies. We plot  $V(L, N)$  versus  $N$  in Fig. 4 for various drives and system sizes. Evidently, the violation of Eq. (3) increases in magnitude with increasing drive. For  $L$  even, the violation first increases with density and then its modulus diminishes. For  $L$  odd, the magnitude of the violation increases monotonically with  $N$ .

Figure 5 shows the difference between thermodynamic and Shannon entropies near equilibrium. The points show values computed directly from the stationary distribution, while the curves are fourth-degree polynomial fits. For small values of the drive, the difference between is  $\propto D^2$ , as expected on grounds of symmetry.

A key question is whether the observed violations persist in larger systems. A preliminary idea is afforded by plotting  $V(L, N)$  versus density at fixed drive, for the four system sizes studied, as in Fig. 6. Evidently, the violation is roughly independent of system size at low densities, while there is a tendency for it to grow with system size at higher densities. Thus, although we are unable to calculate the

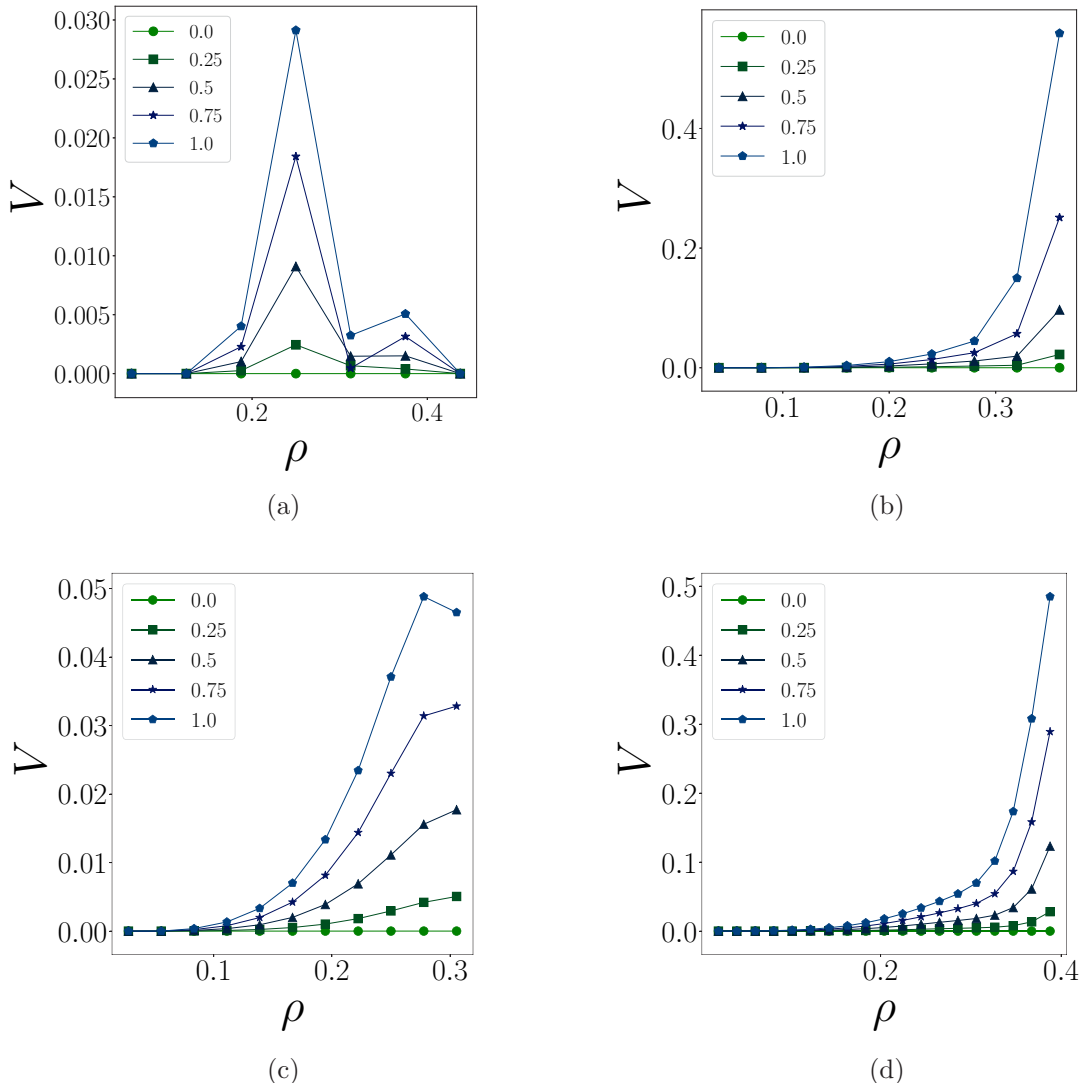


FIG. 4. NNE lattice gas: violation  $V$ , Eq. (16) vs density  $\rho = N/L^2$ , for system sizes  $L = 4-7$  [panels (a)-(d), respectively]. Symbol keys denote the drive parameter  $D$ ; there is no violation for  $D = 0$  (equilibrium).

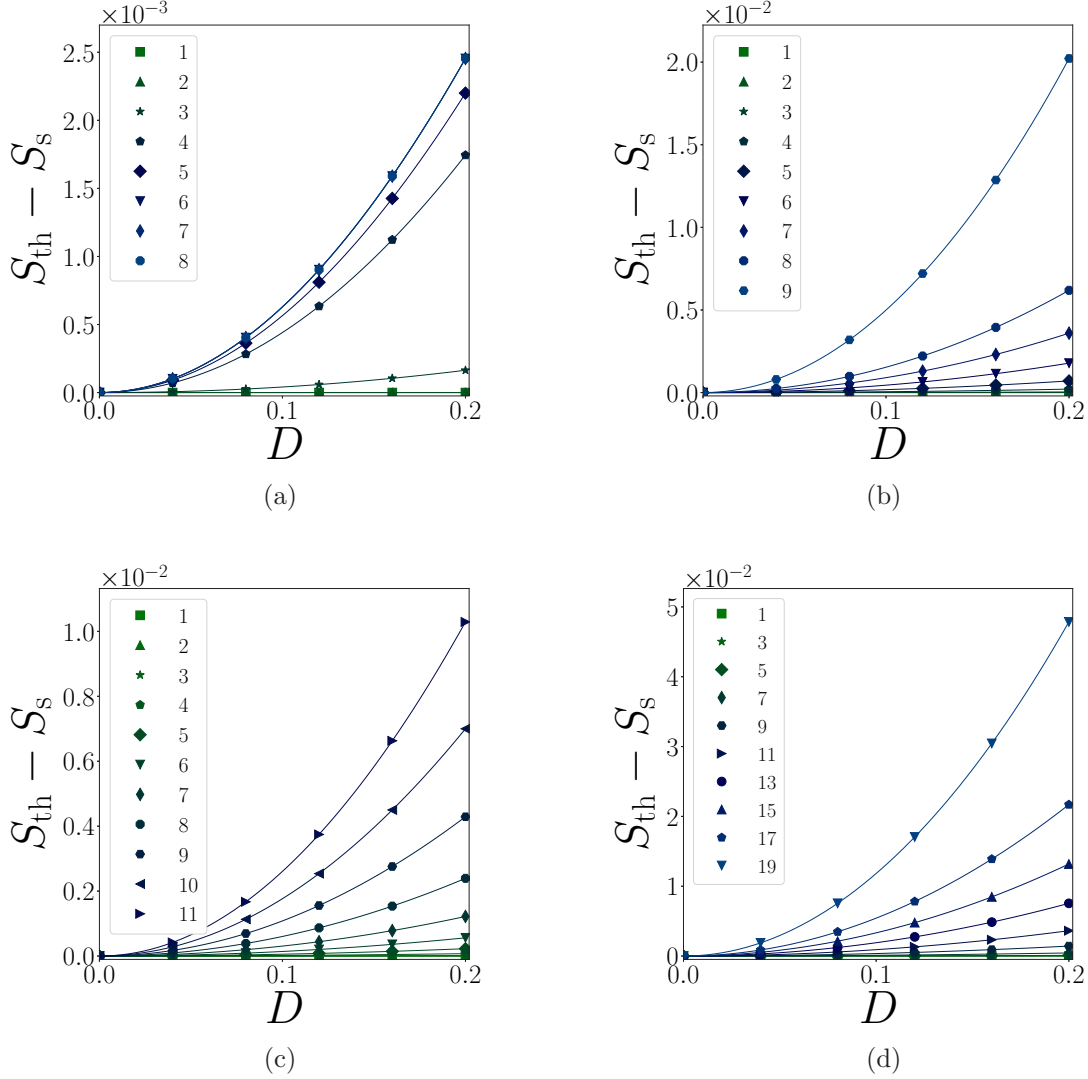


FIG. 5. NNE lattice gas: difference between  $S_{th}$  and  $S_S$  for small drive  $D$ . System sizes  $L = 4-7$  [panels (a)–(d), respectively]. Symbol keys denote the particle number  $N$ . Curves are fourth-degree polynomial fits to the data.

Shannon entropy for  $L > 7$ , we find no evidence that, out of equilibrium, the difference between it and  $S_{th}$  diminishes with increasing system size.

### B. KLS lattice gas

We study the KLS lattice gas on systems of  $4 \times 4$  sites with periodic boundaries, obtaining the stationary solution to the master equation as described in Sec. IV. We verify equality of the thermodynamic and nominal temperatures, and of  $S_{th}$  and  $S_S$ , for zero drive. Under a nonzero drive, however, they are different. Note that Eq. (1) determines  $S_{th}$  to within an additive constant. We choose the latter by setting the two entropies equal in the high-temperature limit, i.e.,  $\lim_{T \rightarrow \infty} S_{th} = \lim_{T \rightarrow \infty} S_S = L^2 \ln 2$ , since in this limit the effect of the drive is null.

In Fig. 7 we compare  $S_{th}$  and  $S_S$  as functions of the energy. Evidently, in the presence of a drive, the thermodynamic entropy exceeds its equilibrium value  $S_{eq}(E)$ , while the Shannon entropy is smaller than  $S_{eq}(E)$ ; the difference grows with increasing drive. For small drives, the difference between

thermodynamic and Shannon entropies is proportional to  $D^2$  (see Fig. 7, inset). The results shown in Fig. 7 are for a system of  $N = 8$  particles (half filling); we find similar results for  $N = 4$  and  $N = 12$ .

We turn next to a test of path independence, as expressed in Eq. (10). We denote the l.h.s. of this equation, which expresses the difference in  $S_{th}$  between systems at the same thermodynamic temperature, but with different particle numbers, by  $\Delta S$ , and the r.h.s., which represents the entropy difference calculated using the chemical potential, by  $\Delta S^*$ . Figure 8 shows the entropy differences versus inverse thermodynamic temperature  $\beta$  in a system of eight particles, for  $D = 0$  and  $D = 1$ . While  $\Delta S$  and  $\Delta S^*$  agree perfectly in equilibrium, there are substantial differences for nonzero drive. We verify that the discrepancy,  $\Delta S - \Delta S^*$ , is proportional to  $D^2$  for small drive.

### C. Two-temperature Ising model

We study the TTI on systems of  $4 \times 4$  sites, integrating Eq. (1) (with  $T$  the thermodynamic temperature), to obtain

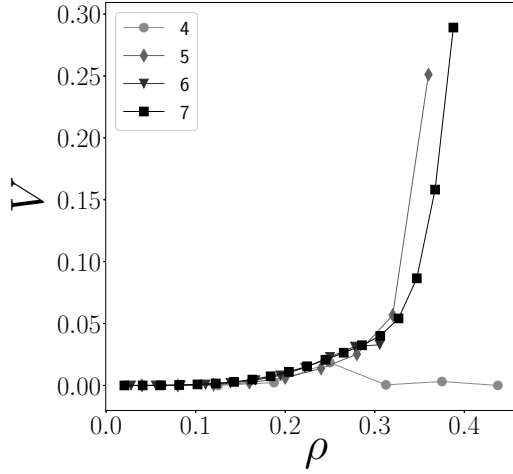


FIG. 6. NNE lattice gas: violation  $V$  vs density  $\rho$  for drive  $D = 0.75$  and system sizes as indicated.

$S_{th}(T, D)$ ; the Shannon entropy is calculated directly from the stationary probability distribution. In these studies we maintain  $T_B/T_A \equiv \alpha$  constant over the path of integration. As in the KLS model, we choose the additive constant in  $S_{th}$  by setting  $S_{th} = S_S$  in the infinite-temperature limit. In this limit we find  $E = -C/T_A$  and  $T = C'/T_A$ , where  $C$  and  $C'$  are  $\alpha$ -dependent constants, leading to  $S_{th} \simeq \lim_{T \rightarrow \infty} S_S - \mathcal{O}(1/T^2)$ .

The two entropies are compared in Fig. 9. For  $T_A = T_B$  we find  $S_{th} = S_S$  as expected, but for unequal temperatures the thermodynamic and Shannon entropies are unequal. Surprisingly, the Shannon entropy is a nonconcave function of energy for  $T_B = 5T_A$  (see Fig. 9, inset). By contrast, concavity of  $S_{th}$  follows from the energy being an increasing function of the thermodynamic temperature  $T$ , as verified numerically. (We have not observed concavity violations of the Shannon entropy in the other models studied.) We verify that  $|S_{th} - S_S| \propto (T_B - T_A)^2$ .

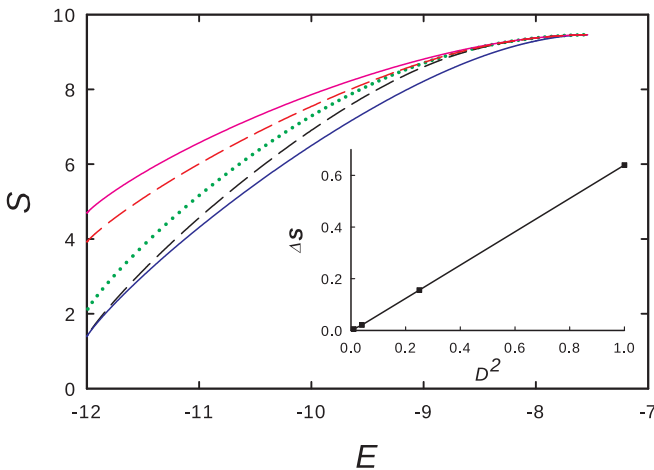


FIG. 7. KLS lattice gas: thermodynamic and Shannon entropies vs energy for a system of  $N = 8$  particles on a square lattice of 16 sites. Continuous curves:  $S_{th}$  (upper) and  $S_S$  (lower) for drive  $D = 10$ . Broken curves:  $S_{th}$  (upper) and  $S_S$  (lower) for drive  $D = 1$ . Dotted line: equilibrium entropy. Inset:  $\Delta S \equiv S_{th} - S_S$  vs  $D^2$  for  $E = -10$ .

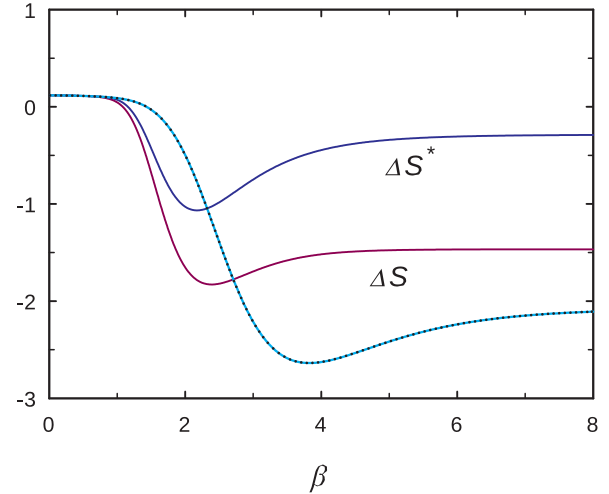


FIG. 8. KLS lattice gas: differences  $\Delta S$  and  $\Delta S^*$  in thermodynamic entropy calculated along two paths vs inverse thermodynamic temperature  $\beta$ , for  $N = 8$  particles on a square lattice of 16 sites. The labeled curves are for drive  $D = 1$ . The superposed dotted and solid curves are for equilibrium, for which  $S_{th}$  is path independent.

We test path independence in the  $T_A$ - $T_B$  plane. For example, consider two paths between the points (3,2) and (4,3) shown in Fig. 10. The change in  $S_{th}$  along path  $a$  is found to be 3.209, whereas that along path  $b$  is 3.253, corresponding to a difference of about 1.4%. Thus path independence is violated in the two-temperature Ising model as well.

It is interesting to note that for a TTI system of just two sites, the thermodynamic and Shannon entropies are equal. In this case the thermodynamic inverse temperature  $\beta = (\beta_A + \beta_B)/2$ , the energy is  $E = -\tanh \beta$ , and  $dS_S/d\beta = dS_{th}/d\beta = -\beta \cosh^{-2} \beta$  (see Appendix B). In larger systems  $\beta$  is not simply the mean of  $\beta_A$  and  $\beta_B$ , and the two entropies are distinct. For a system of four sites, the exact stationary

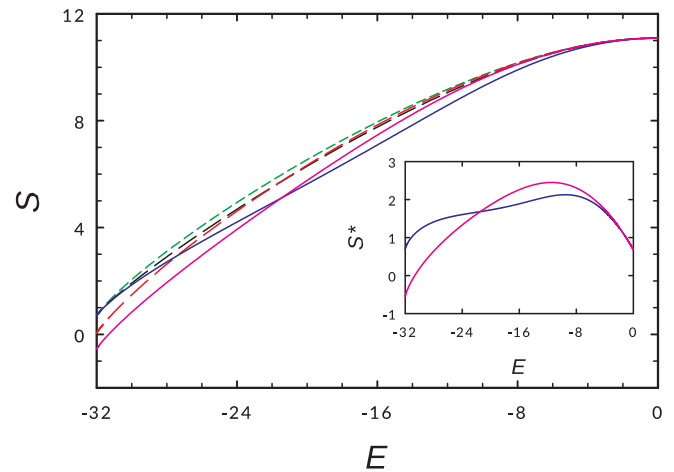


FIG. 9. Two-temperature Ising model on a square lattice of 16 sites. Dashed curves:  $S_{th}$  (lower at left) and  $S_S$  for  $T_B = 2T_A$ . Continuous curves:  $S_{th}$  (lower at left) and  $S_S$  for  $T_B = 5T_A$ . Short dashed curve: equilibrium entropy. Inset: entropies less the overall linear trend,  $S^* \equiv S - 0.3251(E + 32)$  for  $T_B = 5T_A$ ;  $S_{th}^*$  is the lower curve at left.

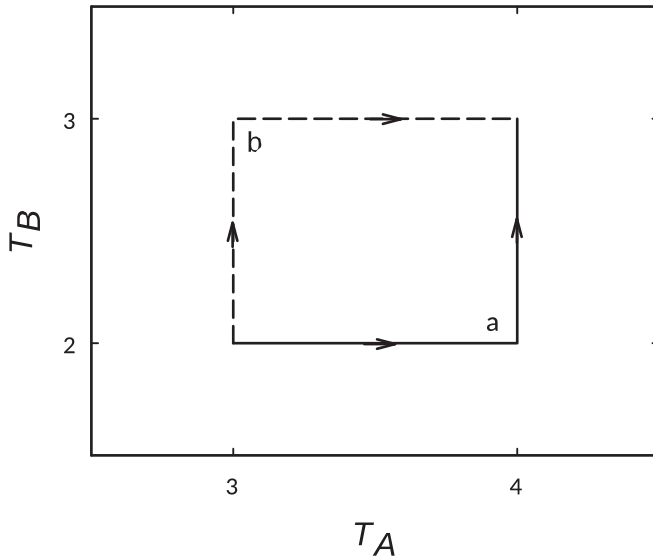


FIG. 10. Paths  $a$  and  $b$  in the  $T_A$ - $T_B$  plane used to calculate  $\Delta S$ .

solution of the master equation is obtained in Appendix B. Evaluating the effective temperature and the change in  $S_{th}$  along the paths shown in Fig. 10, we find that path independence is violated even in this small system, although by only about 0.006%, suggesting that violation of path independence increases with system size. Equivalence of thermodynamic and Shannon entropies is violated in the four-site system.

## V. CONCLUSIONS

We attempt to define a nonequilibrium entropy function  $S_{th}$  via thermodynamic integration. For nonequilibrium steady states in three models that admit consistent definitions of temperature and/or chemical potential using coexistence with a reservoir,  $S_{th}$  differs from the Shannon entropy  $S_S$  of the stationary probability distribution; the difference is proportional to the square of the nonequilibrium parameter, be it drive strength (NNE and KLS models) or the difference between sublattice temperatures (TTI model). Thus, out of equilibrium, the derivative of  $S_S$  with respect to energy does not yield the temperature defined via coexistence, nor does the derivative (or finite difference) of  $S_S$  with respect to particle number yield a chemical potential predictive of coexistence. Adopting some other definition of temperature would imply that equality of temperatures no longer serves as a condition for coexistence between NESS, which goes against the very notion of a thermodynamic temperature. The quantity  $S_{th}$  defined via thermodynamic integration is not a state function out of equilibrium, since it is path dependent. Thus we have failed to find a state function that plays the role of a thermodynamic entropy out of equilibrium.

The NNE and KLS models include a drive, hence a steady particle current, but the TTI has none, so that our findings cannot be ascribed to the presence of a particle current and attendant long-range correlations. Although our numerical technique for determining the stationary probability density (and thus the Shannon entropy) is limited to small systems, the results are significant because (1) there is no reason to

expect thermodynamic integration to yield a state function, or equality of thermodynamic and Shannon entropies, for larger systems; (2) a violation for small systems is still a violation. In equilibrium, the thermodynamic entropy is a state function, equal to the Shannon entropy, and any violation, even for the smallest systems, would be remarkable. Nevertheless, our results do not logically exclude equality of Shannon and thermodynamic entropies in the thermodynamic limit. (Note that such an equivalence would imply that thermodynamic integration yields a state function in this limit.) We hope to address this point in future work.

Our results show that the thermodynamics of nonequilibrium systems (even in steady states) is fundamentally different from that of equilibrium. Indeed, the Shannon entropy can be a nonconcave function of energy in the two-temperature Ising model, a fact that calls into question its use in thermodynamic analyses. (Note that the violation of concavity in no way depends on our definitions of  $T$  or  $S_{th}$ ; these quantities are not involved in calculating  $S_S$ .) Since the Shannon entropy provides the link between thermodynamics and information theory, the nature of this connection for far-from-equilibrium systems is unclear.

We believe the failure to define a steady-state entropy stems from the fact that, out of equilibrium, the stationary probability distribution on configuration space is not of the canonical form, i.e.,  $P(C) \neq (1/Z) \exp[-E(C)/T]$ . It is this relation (in the canonical ensemble, and analogous ones in the other ensembles) that leads to equality of thermodynamic and information entropies. A nonequilibrium drive (essentially by definition) alters the stationary probability distribution so it cannot be written in canonical form.

Recently, Guioth and Bertin [32] showed that in the weak-exchange limit it is possible to define a chemical potential for NESS, provided the particle-exchange dynamics between systems takes a factorized form; inconsistencies arise when it does not [33]. Our study shows that even when the Guioth-Bertin conditions are satisfied, the entropy obtained via thermodynamic integration may not be a state function, and that it differs from the Shannon entropy.

Summarizing, a simple, physically motivated approach to defining an entropy for nonequilibrium steady states is found to be inviable. At the same time, maximization of the Shannon entropy does not predict coexistence out of equilibrium. The question of whether a thermodynamic entropy can be defined far from equilibrium remains unanswered.

## ACKNOWLEDGMENT

This work was supported by CNPq and Capes, Brazil.

## APPENDIX A: CHEMICAL POTENTIAL FOR SMALL SYSTEMS

The relation between temperature, energy, and entropy expressed in Eq. (1) can be applied directly to the KLS and TTI. The case of the lattice gas with NN exclusion demands more care, since we work with a fixed number of particles  $N$ . In the large- $L$  limit, the chemical potential of an athermal



lattice gas, driven or not, is defined so [23]

$$\mu = k_B T \ln \frac{\rho}{\rho_{op}}, \quad (\text{A1})$$

where  $\rho$  is the fraction of occupied sites, and  $\rho_{op}$  is the stationary average density of open sites (i.e., vacant sites at which a particle can be inserted without violating excluded-volume conditions), over configurations with  $N = \rho L^d$  particles. The above relation follows from coexistence with a particle reservoir, is equivalent to the general definition proposed by Sasa and Tasaki [14], and is consistent with the zeroth law of thermodynamics, as verified in [23].

The relation between entropy and chemical potential is  $(\partial S / \partial N)_{E,V} = -\mu^*$ . For a small system, however, the derivative should be replaced with a finite difference, i.e.,  $\Delta S \equiv S(N, E, V) - S(N-1, E, V)$ . Consider an equilibrium athermal system of size  $L$  containing a fixed number  $N$  of particles. Denoting the number of distinct configurations by  $\Omega(L, N)$ , and noting that in equilibrium all such configurations are equally probable, we have

$$S(L, N) = \ln \Omega(L, N), \quad (\text{A2})$$

and

$$\Delta S(L, N) = \ln \frac{\Omega(L, N)}{\Omega(L, N-1)}. \quad (\text{A3})$$

(Recall that we have set Boltzmann's constant to unity.)

Let  $\Gamma(L, N)$  denote the space of configurations of system  $(L, N)$ , so that  $\Omega(L, N) = |\Gamma(L, N)|$  where  $|\Lambda|$  denotes the cardinality of set  $\Lambda$ . For each configuration  $\mathcal{C} \in \Gamma(L, N)$ , let  $N_{op}(\mathcal{C})$  be the number of open sites. Given a configuration  $\mathcal{C} \in \Gamma(L, N-1)$ , we can form  $N_{op}(\mathcal{C})$  distinct configurations in  $\Gamma(L, N)$  by inserting a particle at one of the open sites. Each of these new,  $N$ -particle configurations can be obtained in  $N$  distinct manners, since removing a particle from such a configuration generates a configuration in  $\Gamma(L, N-1)$  with an open site where the particle was removed. Thus,

$$\Omega(L, N) = \frac{1}{N} \sum_{\mathcal{C} \in \Gamma(L, N-1)} N_{op}(\mathcal{C}). \quad (\text{A4})$$

Introducing the mean number of open sites per configuration in  $\Gamma(L, N-1)$ ,

$$\bar{N}_{op}(L, N-1) \equiv \frac{1}{\Omega(L, N-1)} \sum_{\mathcal{C} \in \Gamma(L, N-1)} N_{op}(\mathcal{C}), \quad (\text{A5})$$

we have

$$\Delta S = -\mu^* = \ln \frac{\bar{N}_{op}(L, N-1)}{N}, \quad (\text{A6})$$

which provides the relation between entropy and particle number in a small athermal system in equilibrium. Equation (A6) is simply the Widom insertion relation [34] specialized to athermal systems. [Dividing numerator and denominator on the r.h.s. by the number of sites, we recover Eq. (A1) in the large- $L$  limit.]

Now, in an athermal lattice gas, all configurations have the same energy, so the chemical potential at fixed drive should depend only on  $N$ ,  $\bar{N}_{op}$ , and  $L$ . The effect of the drive is to favor certain configurations over others. Thus we use Eq. (A6)

to define  $\mu^*$ , but with the mean number of open sites now given by

$$\bar{N}_{op}(L, N-1) = \sum_{\mathcal{C} \in \Gamma(L, N-1)} P(\mathcal{C}) N_{op}(\mathcal{C}). \quad (\text{A7})$$

The thermodynamic entropy  $S_{th}(L, N)$  is obtained by iterating  $\Delta S = \ln[\bar{N}_{op}(L, N-1)/N]$ , where we take  $S(L, 0) \equiv 0$ , as in equilibrium. (The drive cannot alter the entropy if there are no particles for it to act upon.)

We want to know if  $\mu^*$  as defined by Eq. (A6) is proportional to the finite difference of the *Shannon entropy* of the stationary probability distribution,

$$S_S(L, N) \equiv - \sum_{\mathcal{C} \in \Gamma(L, N)} P(\mathcal{C}) \ln P(\mathcal{C}), \quad (\text{A8})$$

that is, if the following relation holds:

$$\begin{aligned} & \sum_{\mathcal{C} \in \Gamma(L, N)} P(\mathcal{C}) \ln P(\mathcal{C}) - \sum_{\mathcal{C} \in \Gamma(L, N-1)} P(\mathcal{C}) \ln P(\mathcal{C}) \\ &= \ln \frac{\bar{N}_{op}(L, N-1)}{N}. \end{aligned} \quad (\text{A9})$$

(Note that in the two terms on the l.h.s. of the expression above,  $P(\mathcal{C})$  refers to two different steady states, one having  $N$  particles, the other,  $N-1$ .) This is the relation that we test numerically.

For a nonathermal lattice gas with nearest-neighbor interactions on a hypercubic lattice of  $L^d$  sites in  $d$  dimensions, we have

$$\mu^*(\beta, N, L) = -\ln \frac{Z(\beta, N, L)}{Z(\beta, N-1, L)}, \quad (\text{A10})$$

where  $Z$  denotes the canonical partition function. Now consider the quantity  $g$  defined in Sec. II:

$$\begin{aligned} g &= \sum_{j=0}^q \rho^-(j) e^{-\beta j} = \frac{1}{L^d} \sum_{j=0}^q \frac{e^{-\beta j}}{Z(\beta, N, L)} \sum_{\mathcal{C} \in \Gamma(L, N)} e^{-\beta E(\mathcal{C})} \\ &\times \sum_{i|\sigma_i=1} \delta_{n(i), j}, \end{aligned} \quad (\text{A11})$$

where the final sum is over occupied sites in configuration  $\mathcal{C}$  and  $n(i)$  is the number of occupied nearest neighbor of site  $i$ . Noting that when remove a particle with  $j$  occupied neighbors from configuration  $\mathcal{C} \in \Gamma(L, N)$ , we obtain a configuration  $\mathcal{C}' \in \Gamma(L, N-1)$  with energy  $E(\mathcal{C}') = E(\mathcal{C}) + j$ , we may write

$$\begin{aligned} gZ(\beta, N, L) &= \frac{1}{L^d} \sum_{\mathcal{C} \in \Gamma(L, N)} \sum_{j=0}^q \sum_{i|\sigma_i=1} \delta_{n(i), j} e^{-\beta E(\mathcal{C})} \\ &= \frac{N}{L^d} \sum_{\mathcal{C}' \in \Gamma(L, N)} e^{-\beta E(\mathcal{C}')}. \end{aligned} \quad (\text{A12})$$

Finally, we note that each configuration  $\mathcal{C}' \in \Gamma(L, N-1)$  can be obtained in  $N$  distinct ways by removing a particle from a configuration  $\mathcal{C} \in \Gamma(L, N)$ , whereas each configuration in  $\Gamma(L, N)$  can be generated in  $L^d - (N-1)$  ways by adding a particle to a configuration in  $\Gamma(L, N-1)$ . Thus the sum over  $\mathcal{C} \in \Gamma(L, N)$  in the r.h.s. of Eq. (A12) is

$[L^d - (N - 1)]Z(\beta, N - 1, L)/N$ , so that

$$g = \left(1 - \frac{N-1}{L}\right) \frac{Z(\beta, N-1, L)}{Z(\beta, N, L)}, \quad (\text{A13})$$

and

$$\mu^*(\beta, N, L) = \ln \frac{g}{1 - \frac{N-1}{L^d}}. \quad (\text{A14})$$

### APPENDIX B: TWO-TEMPERATURE ISING MODEL: SYSTEMS OF TWO AND FOUR SPINS

*Two-site system.* Consider a pair of coupled Ising spins,  $\sigma_1$  and  $\sigma_2$  coupled to reservoirs at inverse temperatures  $\beta_A$  and  $\beta_B$ , respectively. The configurations are  $\mathcal{C}_1 = (+, +)$ ,  $\mathcal{C}_2 = (+, -)$ ,  $\mathcal{C}_3 = (-, +)$ , and  $\mathcal{C}_4 = (-, -)$ , with energies  $E_1 = E_4 = -1$  and  $E_2 = E_3 = +1$ . Letting  $\kappa_i = \exp[\beta_i]$ , the master equation for the probabilities  $p_j$  ( $j = 1, \dots, 4$ ) can be written

$$\begin{aligned} \dot{p}_1 &= \kappa_B p_2 + \kappa_A p_3 - w_1 p_1, \\ \dot{p}_2 &= \kappa_A^{-1} (p_1 + p_4) - w_2 p_2, \\ \dot{p}_3 &= \kappa_B^{-1} (p_1 + p_4) - w_2 p_3, \\ \dot{p}_4 &= \kappa_A p_2 + \kappa_B p_3 - w_1 p_4, \end{aligned} \quad (\text{B1})$$

where  $w_1 = \kappa_A^{-1} + \kappa_B^{-1}$  and  $w_2 = \kappa_A + \kappa_B$ . Symmetry implies that the stationary probabilities  $\bar{p}_j$  satisfy  $\bar{p}_1 = \bar{p}_4$  and  $\bar{p}_2 = \bar{p}_3$ . One readily verifies that

$$\bar{p}_1 = \frac{1}{2(1 + \kappa_A^{-1} \kappa_B^{-1})} \quad (\text{B2})$$

and

$$\bar{p}_2 = \frac{\kappa_A^{-1} \kappa_B^{-1}}{2(1 + \kappa_A^{-1} \kappa_B^{-1})}. \quad (\text{B3})$$

The mean energy in the stationary state is

$$\bar{E} = -\frac{1 - e^{-(\beta_A + \beta_B)}}{1 + e^{-(\beta_A + \beta_B)}} = -\tanh \beta, \quad (\text{B4})$$

if we take  $\beta = (\beta_A + \beta_B)/2$ , the average of the two inverse temperatures. This simple expression for the effective inverse temperature arises from the fact that the Boltzmann factors  $\exp[-\beta_A]$  and  $\exp[-\beta_B]$  enter the stationary probability distribution in a multiplicative manner. In this simple case, the thermodynamic temperature is in fact  $T = 1/\beta$ . To see this, consider the stationary energy flux  $J_E$  between the system and a reservoir at temperature  $T$ . Considering all eight possible transitions, we have

$$J_E = 4\bar{p}_1 e^{-\beta} - 4\bar{p}_2 e^{\beta} = 0, \quad (\text{B5})$$

because  $\bar{p}_1 = e^{2\beta} \bar{p}_2$ .

*Four-site system.* We consider the TTI on a lattice of  $2 \times 2$  sites. Using symmetries, the configurations are found to fall into five distinct equivalence classes, listed in Fig. 11 along with their associated configuration numbers  $\omega$  and the classes accessible from each class. Consider class  $a$ . From the figure, one sees that a configuration in this class is accessible via two transitions from configurations in class  $b$ , and two in class  $c$ . The associated transition rates are  $e^{2\beta_A} \equiv \kappa_A$  and

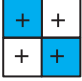
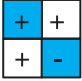
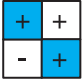
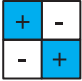
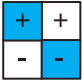
Class	Conf.	$\omega$	In/Out
a		2	b(2), c(2)
b		4	a, d, e(2)
c		4	a, d, e(2)
d		2	b(2), c(2)
e		4	b(2), c(2)

FIG. 11. Configuration classes and transitions for the TTI model on a lattice of  $2 \times 2$  sites. For each of the five classes, a representative configuration is shown, followed by the number  $\omega$  of configurations in the class. The final column (In/Out) lists the classes accessible from the given class, and from which it is accessible. The number 2 in parentheses indicates that there are two distinct transitions between the classes. Squares with light color: sublattice A; white squares: sublattice B.

$e^{2\beta_B} \equiv \kappa_B$ , respectively. A configuration in class  $a$  can make transitions to classes  $b$  and  $c$  (there are again two distinct transitions in each case), with associated rates  $\kappa_A^{-1}$  and  $\kappa_B^{-1}$ , respectively. Enumerating the transitions in this manner, we arrive at the following set of equations of motion, in which the probabilities of a representative configuration of classes  $a, b, \dots, e$  are denoted by  $\alpha, \beta, \dots, \epsilon$ :

$$\dot{\alpha} = 2\kappa_A \beta + 2\kappa_B \gamma - 2(\kappa_A^{-1} + \kappa_B^{-1})\alpha, \quad (\text{B6})$$

$$\dot{\beta} = \kappa_A^{-1} \alpha + \kappa_A \delta + 2\epsilon - (2 + \kappa_A + \kappa_A^{-1})\beta, \quad (\text{B7})$$

$$\dot{\gamma} = \kappa_B^{-1} \alpha + \kappa_B \delta + 2\epsilon - (2 + \kappa_B + \kappa_B^{-1})\gamma, \quad (\text{B8})$$

$$\dot{\delta} = 2\kappa_A^{-1} \beta + 2\kappa_B^{-1} \gamma - 2(\kappa_A + \kappa_B)\delta, \quad (\text{B9})$$

$$\dot{\epsilon} = 2\gamma + 2\beta - 4\epsilon. \quad (\text{B10})$$

Using the normalization condition,  $\sum_i \omega_i p_i = 1$ , straightforward algebra leads to the stationary solution:

$$\alpha^* = \frac{\kappa_A \kappa_B (\kappa_A^2 \kappa_B^2 + \kappa_A^2 \kappa_B + \kappa_A \kappa_B^2 + \kappa_A^2 - \kappa_A \kappa_B + \kappa_B^2)}{W(\kappa_A, \kappa_B)}, \quad (\text{B11})$$

$$\beta^* = \frac{\kappa_A (\kappa_B^3 + \kappa_B^2 + \kappa_A \kappa_B + \kappa_A)}{W(\kappa_A, \kappa_B)}, \quad (\text{B12})$$

$$\gamma^* = \frac{\kappa_B (\kappa_A^3 + \kappa_A^2 + \kappa_A \kappa_B + \kappa_B)}{W(\kappa_A, \kappa_B)}, \quad (\text{B13})$$

$$\delta^* = \frac{\kappa_A^2 - \kappa_A \kappa_B + \kappa_A + \kappa_B^2 + \kappa_B + 1}{W(\kappa_A, \kappa_B)}, \quad (\text{B14})$$

$$\epsilon^* = \frac{\kappa_A^3 \kappa_B + 2\kappa_A^2 \kappa_B + \kappa_A^2 + \kappa_A \kappa_B^3 + 2\kappa_A \kappa_B^2 + \kappa_B^2}{2W(\kappa_A, \kappa_B)}, \quad (\text{B15})$$

where

$$\begin{aligned} W(\kappa_A, \kappa_B) = & 2\kappa_A^3 \kappa_B^3 + 2\kappa_A^3 \kappa_B^2 + 8\kappa_A^3 \kappa_B + 2\kappa_A^2 \kappa_B^3 - 2\kappa_A^2 \kappa_B^2 \\ & + 12\kappa_A^2 \kappa_B + 8\kappa_A^2 + 8\kappa_A \kappa_B^3 + 12\kappa_A \kappa_B^2 - 2\kappa_A \kappa_B \\ & + 2\kappa_A + 8\kappa_B^2 + 2\kappa_B + 2. \end{aligned} \quad (\text{B16})$$

- [1] U. Seifert, Entropy Production along a Stochastic Trajectory and an Integral Fluctuation Theorem, *Phys. Rev. Lett.* **95**, 040602 (2005).
- [2] G. E. Crooks, Entropy production fluctuation theorem and the nonequilibrium work relation for free energy differences, *Phys. Rev. E* **60**, 2721 (1999).
- [3] H. Qian, Mesoscopic nonequilibrium thermodynamics of single macromolecules and dynamic entropy-energy compensation, *Phys. Rev. E* **65**, 016102 (2001).
- [4] K. R. Narayanan and A. R. Srinivasa, Shannon-entropy-based nonequilibrium “entropic” temperature of a general distribution, *Phys. Rev. E* **85**, 031151 (2012).
- [5] U. Seifert, Stochastic thermodynamics, fluctuation theorems and molecular machines, *Rep. Prog. Phys.* **75**, 126001 (2012).
- [6] S. Ray, A. Baura, and B. C. Bag, Nonequilibrium entropic temperature and its lower bound for quantum stochastic processes, *Phys. Rev. E* **89**, 032148 (2014).
- [7] C. Van den Broeck and M. Esposito, Ensemble and trajectory thermodynamics: A brief introduction, *Physica A* **418**, 6 (2015).
- [8] T. S. Komatsu, N. Nakagawa, S.-i. Sasa, and H. Tasaki, Exact Equalities and Thermodynamic Relations for Nonequilibrium Steady States, *J. Stat. Phys.* **159**, 1237 (2015).
- [9] H. B. Callen, *Thermodynamics and an Introduction to Thermostatistics*, 2nd ed. (Wiley, New York, 1985).
- [10] T. Tomé and M. J. de Oliveira, Entropy production in irreversible systems described by a Fokker-Planck equation, *Phys. Rev. E* **82**, 021120 (2010).
- [11] T. Tomé and M. J. de Oliveira, Stochastic approach to equilibrium and nonequilibrium thermodynamics, *Phys. Rev. E* **91**, 042140 (2015).
- [12] T. Tomé and M. J. de Oliveira, Entropy Production in Nonequilibrium Systems at Stationary States, *Phys. Rev. Lett.* **108**, 020601 (2012).
- [13] Y. Oono and M. Paniconi, Steady state thermodynamics, *Prog. Theor. Phys. Suppl.* **130**, 29 (1998).
- [14] S.-i. Sasa and H. Tasaki, Steady state thermodynamics, *J. Stat. Phys.* **125**, 125 (2006).
- [15] S. R. Williams, D. J. Searles, and D. J. Evans, On the relationship between dissipation and the rate of spontaneous entropy production from linear irreversible thermodynamics, *Mol. Sim.* **40**, 208 (2014).
- [16] T. Hatano and S.-I. Sasa, Steady-State Thermodynamics of Langevin Systems, *Phys. Rev. Lett.* **86**, 3463 (2001).
- [17] K. Hayashi and S.-i. Sasa, Thermodynamic relations in a driven lattice gas: Numerical experiments, *Phys. Rev. E* **68**, 035104(R) (2003).
- [18] E. Bertin, K. Martens, O. Dauchot, and M. Droz, Intensive thermodynamic parameters in nonequilibrium systems, *Phys. Rev. E* **75**, 031120 (2007).
- [19] P. Pradhan, C. P. Amann, and U. Seifert, Nonequilibrium Steady States in Contact: Approximate Thermodynamic Structure and Zeroth Law for Driven Lattice Gases, *Phys. Rev. Lett.* **105**, 150601 (2010).
- [20] P. Pradhan, R. Ramsperger, and U. Seifert, Approximate thermodynamic structure for driven lattice gases in contact, *Phys. Rev. E* **84**, 041104 (2011).
- [21] S. Chatterjee, P. Pradhan, and P. K. Mohanty, Gammalike Mass Distributions and Mass Fluctuations in Conserved-Mass Transport Processes, *Phys. Rev. Lett.* **112**, 030601 (2014).
- [22] S. Chatterjee, P. Pradhan, and P. K. Mohanty, Zeroth law and nonequilibrium thermodynamics for steady states in contact, *Phys. Rev. E* **91**, 062136 (2015).
- [23] R. Dickman and R. Motai, Inconsistencies in steady-state thermodynamics, *Phys. Rev. E* **89**, 032134 (2014).
- [24] R. Dickman, First- and second-order phase transitions in a driven lattice gas with nearest-neighbor exclusion, *Phys. Rev. E* **64**, 016124 (2001).
- [25] S. Katz, J. L. Lebowitz, and H. Spohn, Phase transitions in stationary nonequilibrium states of model lattice systems, *Phys. Rev. B* **28**, 1655 (1983).
- [26] B. Schmittmann and R. K. P. Zia, in *Statistical Mechanics of Driven Diffusive Systems*, Phase Transitions and Critical Phenomena Vol. 17, edited by C. Domb and J. L. Lebowitz (Academic, London, 1995).
- [27] J. Marro and R. Dickman, *Nonequilibrium Phase Transitions in Lattice Models* (Cambridge University Press, Cambridge, UK, 1999).
- [28] H. W. J. Blöte, J. R. Heringa, A. Hoogland, and R. K. P. Zia, Critical properties of non-equilibrium systems without global currents: Ising models at two temperatures, *J. Phys. A* **23**, 3799 (1990).
- [29] J. R. Heringa, H. W. J. Blöte, and A. Hoogland, Critical properties of 3D Ising systems with non-Hamiltonian dynamics, *Int. J. Mod. Phys. C* **05**, 589 (1994).
- [30] R. Dickman, Numerical analysis of the master equation, *Phys. Rev. E* **65**, 047701 (2002).
- [31] R. Dickman, Absorbing-state phase transitions: Exact solutions of small systems, *Phys. Rev. E* **77**, 030102(R) (2008).
- [32] J. Guioth and E. Bertin, Large deviations and chemical potential in bulk-driven systems in contact, *Europhys. Lett.* **123**, 10002 (2018).
- [33] R. Dickman, Failure of steady-state thermodynamics in nonuniform driven lattice gases, *Phys. Rev. E* **90**, 062123 (2014).
- [34] B. Widom, Some topics in the theory of fluids, *J. Chem. Phys.* **39**, 2808 (1963).